GEOLOGY AND GEOPHYSICS OF THE ZUNIL GEOTHERMAL SYSTEM, GUATEMALA

Duncan Foley(1), Joseph N. Moore(2), Susan J. Lutz(2), Julio C. Palma A.(3), Howard P. Ross(2), Edgar Tobias G.(4), and Alan C. Tripp(2)

(1) Pacific Lutheran University, Department of Earth Sciences, Tacoma WA 98447
(2) University of Utah Research Institute, Salt Lake City, UT 84108
(3) Instituto Nacional de Electricificacíon, Guatemala City, Guatemala
(4) Instituto Nacional de Electricificacíon, Guatemala City, Guatemala

ABSTRACT

The Zunil geothermal system in western Guatemala is located adjacent to the active volcanic centers of Santa Maria and Cerro Quemado, where the northeast-trending Zunil fault system transects the proposed Quetzaltenango caldera. The volcanic and intrusive host rocks of the geothermal system are highly altered, with the degree of alteration and veining increasing with depth. The effects of hydrothermal alteration are reflected in both the resistivity and gravity data. The electrical soundings define the presence of a resistive basement at depths of 200-400 m that correlates with a change in the clay mineralogy of the volcanic rocks. Trends in conductivity-thickness products also may reflect an increase in the development of electrically conductive clays away from the upwelling center. Hydrothermal alteration may be reflected in the gravity data as low amplitude gravity highs. Both the field mapping and gravity studies define a series of northwest- and northeast-trending faults.

INTRODUCTION

The Zunil geothermal system is located about 200 km west of Guatemala City, Guatemala, and approximately 10 km southeast of the city of Quetzaltenango (Fig. 1). Six deep wells and eleven thermal-gradient wells have been drilled to date. The highest measured temperature is 288°C; the deepest well is 1310 m. Recent reservoir tests on the existing wells indicate a production capacity of at least 7.3 MW (Menzies et al., 1990). The studies described in this paper were undertaken to help site a series of new production wells.

REGIONAL GEOLOGY

Active subduction of oceanic crust beneath Guatemala has generated both the volcanism that produces heat for the Zunil geothermal system and regional and local systems of tectonic fractures that allow circulation of hydrothermal fluids. Active stratovolcanoes (such as Santa Maria; Rose, 1987), extensive

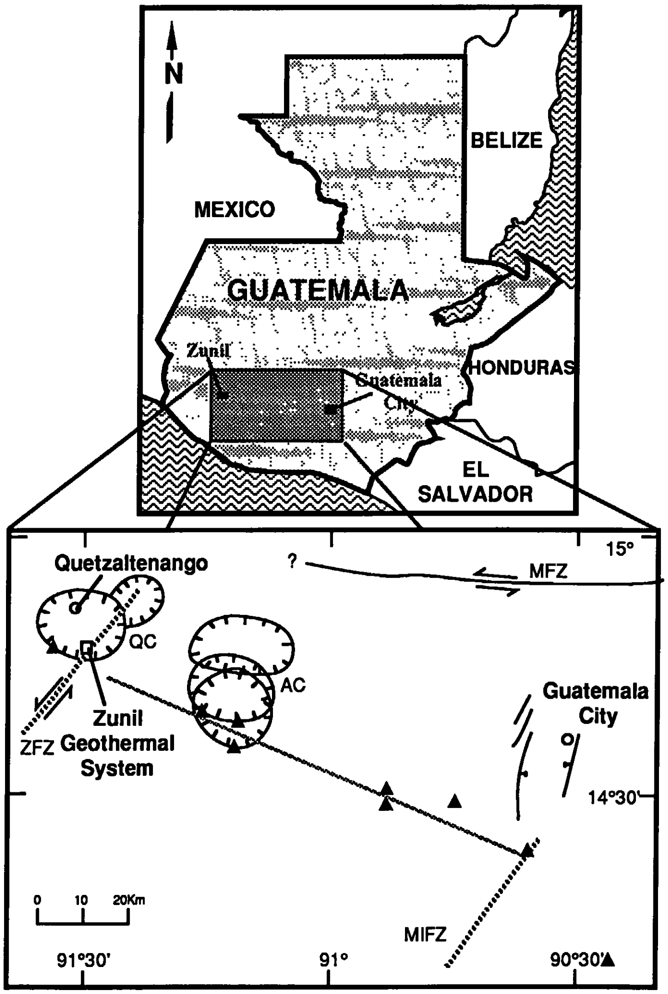

Figure 1. Regional location map of the Zunil geothermal system and the proposed Quetzaltenango caldera (QC). Calderas are shown with hatchures (AC-Atitlan calderas of Newhall, 1987); triangles represent active stratovolcanoes; selected faults near Guatemala City are shown with the ball on the downthrown side; major regional fault zones are shown as dotted lines (ZFZ-Zunil fault zone; MIFZ-Mexico fault zone; MFZ Motagua fault zone.) Modified from Newhall (1987).

northeast-trending crustal fractures (e.g., Stoiber and Carr, 1973), and large calderas (e.g., Newhall, 1987) are found throughout the highlands of southern and southwestern Guatemala.

Figure 1 shows the location of the Zunil geothermal system and some of the more important tectonic and volcanic features of south-central Guatemala. Geologic mapping and satellite-image interpretation show that the geothermal field is located on the southern margin of a circular feature that we suggest represents the ring structure of a large caldera.

Definitive proof for the existence of this caldera (which herein is referred to as the "Quetzaltenango Caldera") is beyond the scope of this study. The caldera hypothesis is attractive, however, because it explains the regional setting of the Zunil geothermal field, and provides a framework for the interpretation of volcanologic, topographic, and geophysical features in the region (Grant Heikan, personal communication, 1989). Figure 1 also shows the locations of major stratovolcanoes, which define a northwest trend, and regional northeast-trending zones of crustal weakness.

Although seemingly large, the size of the proposed Quetzaltenango caldera is equivalent to the Atitlan calderas (Fig. 1) identified by Newhall (1987). Its scale and history may, upon further inspection, be found to parallel other multiple calderas in Guatemala. No regional ash-flow sheets have yet been correlated with the proposed Quetzaltenango caldera. However, there are thick deposits of ash-flow tuff between Quetzaltenango and Huehuetenango which have no known source (Samuel Bonis, personal communication, 1989). The occurrence of these deposits is consistent with the proposed caldera. It is interesting to note that the proposed Quetzaltenango caldera is located at the intersection of major northeast and northwest regional tectonic trends. Tobias and Quiesa (1981) have obtained dates of 1.8 my to 2.5 my from volcanic rocks outside the caldera; these dates may represent the times of the major caldera-forming eruptions.

Younger volcanoes and calderas with reported dates of 660,000 y to as recent as 1818 (Tobias and Quiesa, 1981; Rose, 1987) fill the overall depression of the Quetzaltenango caldera as resurgent domes and flows (Fig. 2). This is typical of many other calderas around the world, and has resulted in a present-day topography that is much different from its original shape. Rose (1987) identified many of these features in his discussion of the prestratocone topography and geology at Volcan Santa Maria, including Las Majadas. Volcan Santiaguito (Fig. 2), located southwest of the proposed caldera boundary, is currently active.

Northeast fault trends are related to the Zunil fault zone (Williams, 1960), which has been identified as a zone of predominantly left-lateral strike-slip motion (Stoiber and Carr, 1973). The Zunil fault system consists of several subparallel faults which define a zone as much as 10 kilometers across (Fig. 2).

Perhaps the largest scale northeast-trending feature shown in Fig. 2 is the volcanic alignment of Volcan Santiaguito, Volcan Santa Maria, and the closely paired vents of Cerro Candelaria and Cerro Quemado. This alignment also includes Volcan del Valle (Rose, 1987) and several individual vents on the south slopes of Cerro Candelaria (Tobias and Quiesa, 1981; Johns, 1975). Extending north, the alignment includes several volcanic vents identified by Tobias and Quiesa (1981) on the western margin of the Almolonga caldera. The northeast trend is also reflected in the alignment of other volcanoes, individual fault and joint trends, river courses, and regional fracture systems.

Numerous northeast- and northwest-trending faults have been mapped within the well field at Zunil (Fig. 3). These faults, which have offsets that may range up to several hundreds of meters, form a complex series of horsts and grabens. Figure 3 shows that many of the fumeroles and springs in the western part of the well field are associated with northeast-trending faults. High concentrations of soil mercury demonstrate that the northern end of the northwestern-trending fault near ZCQ-6 is also highly permeable (Moore, unpublished data). Significantly, no geothermal features are found to the west and southwest of this fault.

Chemical and temperature data suggest that a shallow upwelling center is located in the vicinity of ZCQ-3, 5 and 6. The highest temperatures (288°C) were recorded in ZCQ-5 and 6 at a depth of approximately 1000 m (Mink et al. 1988; Menzies et al., 1990). Chloride-enthalpy relationships show that the least diluted fluids are produced by wells ZCQ-3 and 6 (Adams et al., 1990). Our mapping indicates that this upwelling center is located in an area of high fracture permeabilities at the intersection of major northeast- and northwest-trending faults near Z-11.

In summary, the Quetzaltenango caldera is typical of many geothermally favorable calderas found throughout the world, such as the Yellowstone and Valles calderas in the USA. At Valles and Yellowstone, major calderas have had several periods of eruption and collapse, and favorable geothermal sites are found where the structural margins of the calderas

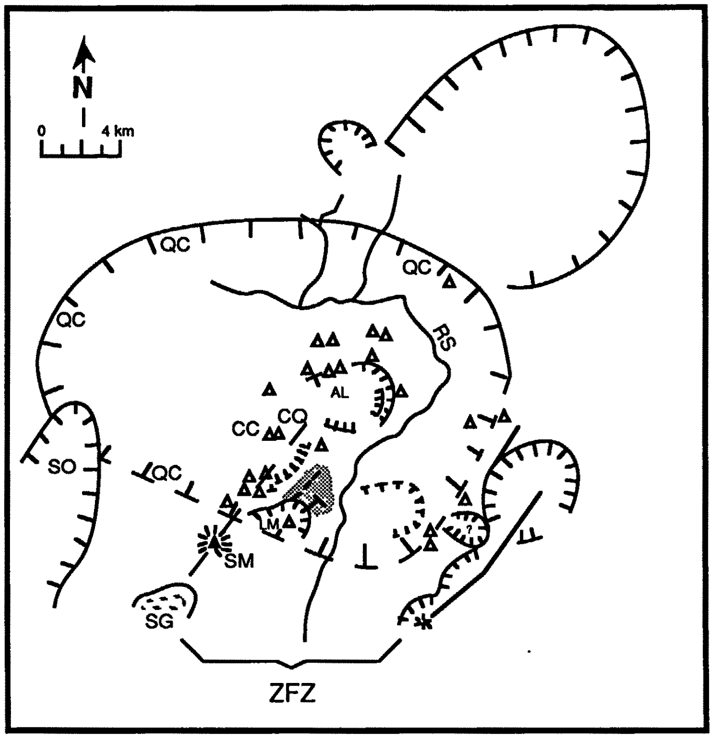

Figure 2. Map of the Zunil area showing the major volcanic features. The Quetzaltenango caldera (QC), Almolonga (AL), Las Majadas (LM), Siete Orejas (SO), and other volcanic depressions are indicated with hatchured lines. Santa Maria (SM) and Santiaguito (SG) volcanoes are shown slightly outside the proposed caldera. Solid triangles indicate younger volcanic vents mapped by Johns (1975) and Tobias and Quiesa (1981); CC = Cerro Candelaria; CQ = Cerro Quemado; RS = Rio Samala. The inferred location of the Zunil fault zone (ZFZ) is bounded by the solid and dashed lines. The western boundary of this fault zone passes through Santa Maria. The eastern boundary is defined by the axis of the volcanic depressions east of the Quetzaltenango caldera. The shaded area shows the location of the Zunil well field.

have been further fractured by regional fault zones. At Valles (Goff et al., 1989), the geothermal system is found in and adjacent to the caldera, along faults related to the regional Jemez fault zone and to volcanic activity in the caldera. At Yellowstone (Smith and Braile, 1984; Christiansen and Hildreth, 1989) geothermal (and younger volcanic) activity is concentrated along the margins of resurgent domes, in areas where the caldera margin is fractured by regional fault systems, and along the regional fault systems.

The Zunil fault zone is a major break in the side of the Quetzaltenango caldera. Thus, the Zunil geothermal area is regionally located: (1) near the structural margin of the caldera (providing permeability along caldera-margin faults); (2) where the permeability of the regional rocks has been increased by fracture networks related to the Zunil fault zone; (3) adjacent to the young heat source of the Cerro Quemado domes and flows; and (4) at a lower elevation than the potential hydrologic recharge areas of either the Llano de Pinal or the Quetzaltenango Valley (Adams et al., 1990). It therefore is located at the intersection of two major fault zones which are adjacent to and hydrologically downgradient from the young heat source in the area.

STRATIGRAPHY AND ALTERATION

The lithologies encountered in the thermal gradient and production wells at Zunil consist of a thick sequence of lava flows and ash-flow tuffs that unconformably overlie a basement of granodiorite (ELC-Electroconsult, 1980; Tobias, 1978, unpub. lithologic logs). Throughout most of the area, the volcanic rocks are covered by a thin veneer of alluvium, pumiceous deposits, and recent landslide debris.

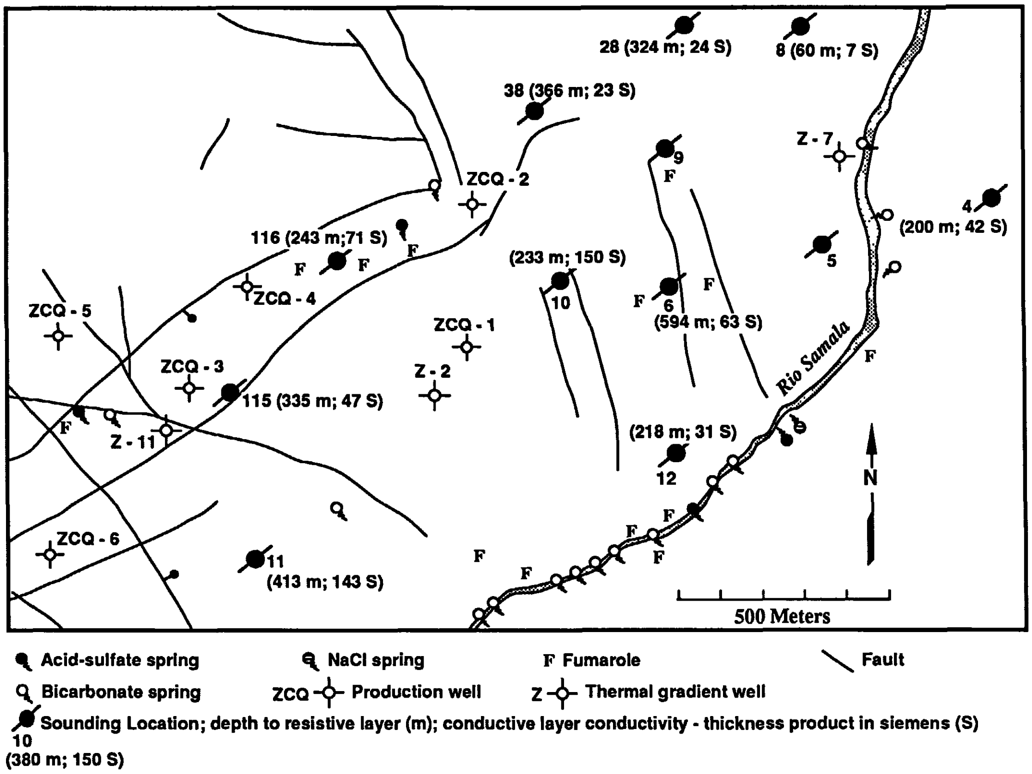

Figure 3. Map of the Zunil well field showing the locations of mapped faults, surface manifestations, wells, and the vertical electrical soundings.

The volcanic rocks can be assigned to four volcanic sequences that range in age from Pleistocene to Tertiary. These include the Galapago Andesite (Pleistocene), Almolonga Volcanics (Pleistocene), Green Tuff (Pliocene), and the Old Zunil Lavas (Pliocene). However, the absolute ages of the rocks have not yet been well established.

The Galapago Andesite consists of a sequence of lava flows that reaches a maximum thickness of 200 m in wells ZCQ-5 and 6. The flows thin to the east, suggesting that they were erupted from a vent located to the west of the well field. The andesite flows are underlain by a thick succession of dacite lava flows, interbedded ash-flow tuffs, and andesite flows of the Almolonga Volcanics. The Almolonga Volcanics have a maximum thickness of 800 m in well ZCQ-3. In wells ZCQ-1, 5, and 6 and Z-11, thin (25-50 m) andesite lava flows separate the Almolonga Volcanics into upper and lower dacite-flow sequences. The contact between the Almolonga Volcanics and the underlying Green Tuff is marked by a lithic-rich ash-flow tuff in wells ZCQ-1, 5, and 6. The Green Tuff is composed of two major units, an upper lithic-rich tuff and a lower welded dacite ash-flow tuff. Both units are highly variable in thickness. The ash-flow tuffs may be part of the eruptive sequence associated with the Quetzaltenango caldera. The oldest volcanic unit encountered in the wells consists of up to 200 m of thinly interbedded andesite and dacite flows of the Old Zunil Lavas.

The base of the volcanic section in ZCQ-3 and 6 is associated with intense veining and lost circulation. In ZCQ-5, the granodiorite displays evidence of brecciation. These relationships indicate that the permeable zones located near the base of these wells are associated with faults.

The hydrothermal alteration can be broadly characterized as argillic or propylitic. Argillic alteration is restricted to the upper 100-200 m of the wells. The rocks in this zone contain smectite, illite-smectite, kaolin, quartz, chalcedony, calcite and zeolites. The rocks underlying the argillic zone can be divided into an upper and a lower propylitic zone. The upper propylitic zone is characterized by traces of epidote, calcite, quartz, and clays. Illite-smectite and chlorite-smectite are the common clay minerals at depths shallower than 300 m whereas illite and chlorite are dominant at greater depths. Little veining has been observed in the upper propylitic zone. Below depths of 500 to 600 m, the rocks commonly contain epidote-bearing veins (lower propylitic zone). The top of the propylitic zone consists of a hydrothermal breccia that is developed in lava flows of the

Galapago Andesite in wells ZCQ-5 and 6 and in dacite flows occurring at the top of the Almolonga Volcanics in well ZCQ-3.

Hydrothermal breccias and the mineral assemblages in wells ZCQ-3, 5 and 6 show that boiling occurred primarily in the volcanic rocks as the fluids moved upward from the granodiorite. Veins within the volcanic rocks consist of calcite + quartz ± epidote ± wairakite. In contrast, veins near the top of the granodiorite are filled with quartz + epidote, suggesting that mineralization occurred in response to cooling. Veins and textures within well ZCQ-1 indicate that boiling has occurred throughout both the volcanic section and granodiorite in this well.

The condensation of steam and CO_2 in the shallow groundwaters has produced a steam-heated cap over the thermal system that has resulted in pervasive but locally intense illitization and the deposition of veins containing illite or albite. Petrographic relationships demonstrate that these veins postdate the propylitic alteration present in the reservoir rocks.

Illite veins and zones of intense illitization are most common in ZCQ-1, where they are present in both the volcanic rocks and the granodiorite. Albite-bearing veins occur in the western part of the well field in wells ZCQ-3, 5 and 6 and Z-11. The distribution of vein albite and illite suggests that the steam-heated reservoir is thickest in the vicinity of ZCQ-1 but thins to the west. These relationships imply that wells ZCQ-3, 5 and 6 are closer to the upwelling center of the geothermal system than well ZCQ-1 (Moore et al., 1990).

A sample of illite, which was expelled from well ZCQ-5 during testing, was dated at $248 \pm 9 \times 10^3$ years. This sample of altered dacite from the Almolonga volcanics fits well within the expected range of dates for post-caldera volcanic activity.

RESISTIVITY STRUCTURE

Approximately 30 Schlumberger soundings (VES) were completed in the vicinity of the well field. The soundings can be divided into two groups. Soundings located to the north and west of the well field indicate high resistivity terrain, with little variation.

The soundings shown in Figure 3 were inverted using the method of Inman (1975). Most soundings could be interpreted with a four layer model. The upper two layers are characterized by high resistivities. These layers are underlain by a thick intermediate layer with low resistivities, which is in turn underlain by a layer with high resistivities. The thickness of the deep resistive layer, however, cannot be resolved from the soundings. In a few cases, interpretation of the data required the presence of additional shallow high resistivity layers. In all cases, these layers are thin.

The nomial depth to the deep resistive layer is indicated in Figure 3. In general, the top of the deep resistive layer appears to be located at depths ranging from 200 to slightly over 400 m. These depths correlate most closely to a change in the secondary mineral assemblages in the nearby wells. In these wells, the rocks in the upper several hundred meters are characterized by conductive clays, including smectite, illite-smectite, and chlorite-smectite. Rocks in the deeper, higher-temperature portions of the well have been altered to less conductive clay minerals such as illite and chlorite.

The conductive-layer parameters were determined through inversion and then varied by a factor of two to evaluate the sensitivity of the interpretations. This indicated that the resistivities and thicknesses of the conductive layers are poorly resolved. Thus, although we are certain that a conductive zone exists, its thickness is largely unresolved from the soundings themselves. This means that the depth to the top of the underlying resistive layer is also poorly resolved.

Even though our analysis of the data has shown that the thicknesses and conductivities of the conductive layer are poorly resolved, the conductivity-thickness product of the layer is always well resolved. Figure 3 gives the values of conductivity-thickness products for the soundings. The conductivity-thickness product or conductance is proportional to the number of charge-carrying ions/anions available in the layer. Figure 3 shows that the conductivity-thickness product increases away from the area around ZCQ-3. An increase in the conductivity-thickness product could result from: 1) an increase in the thickness of the clay-bearing alteration zones; 2) an increase in the abundance of conductive clays; 3) increased porosity; or 4) increased conductivity of the pore fluids. The distribution of the conductivity-thickness product is consistent with the pattern of fluid movement inferred from chemical analyses of well and spring samples (Adams et al., 1990). Chloride-enthalpy relationships indicate that the geothermal fluids cool conductively and by dilution as they move to the east and south away from vicinity of ZCQ-3 and 6. Both cooling and dilution will promote increased development of conductive clay minerals such as smectite.

Although we have interpreted the data using a layered-earth model, many of the data sets show significant multi-dimensional and topographic effects. Slopes steeper than 45° in the ascending branches at large current-electrode spacings for soundings 4, 5, 6, 8, 10, 11, 115, and 116 for example,

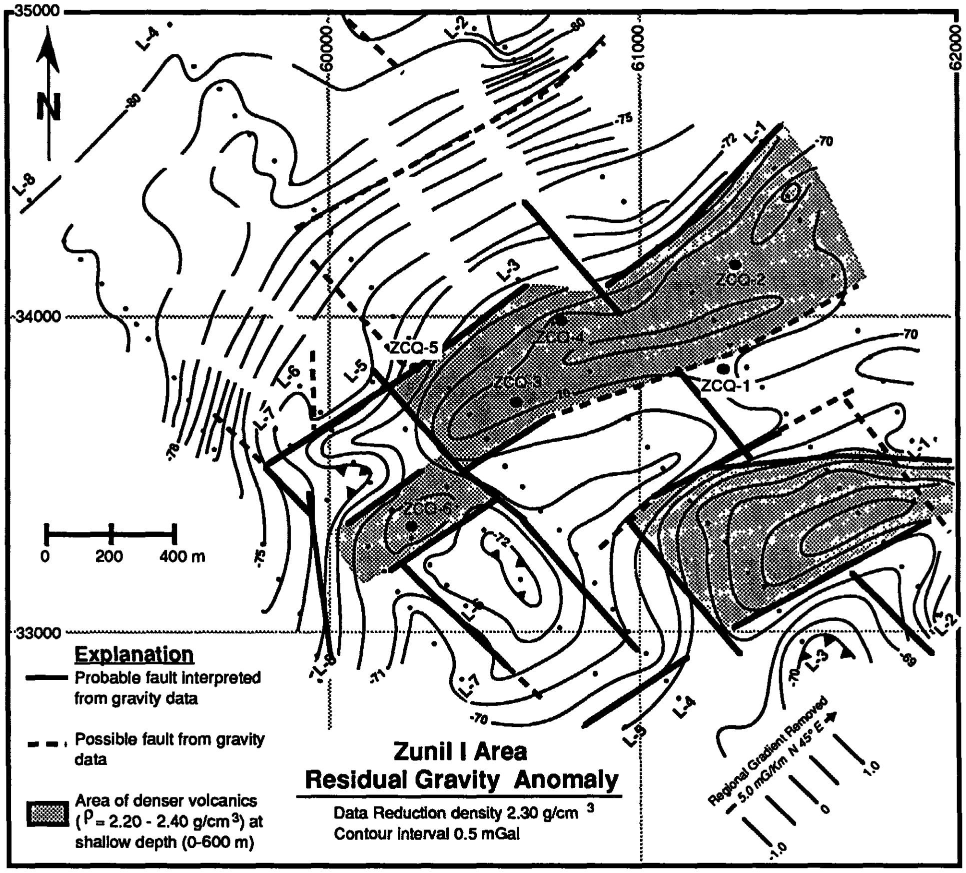

Figure 4. Residual gravity map of the area containing the Zunil well field. See text for discussion.

cannot be produced by any layered earth and indicate the effects of topography and/or lateral resistivity contrasts.

GRAVITY STUDIES

Both regional and detailed gravity surveys were completed by the Instituto Nacional de Electricificacíon in the Zunil area. A regional survey extending from Quetzaltenango to approximately 3 km south of Cerro El Galapago covers an area of approximately 90 sq km. A detailed survey which covers approximately 6 sq km was completed in the area of the well field in August 1989. This survey consisted of eight northwest-trending survey lines with station spacings of approximately 70 to 200 m (Fig. 4).

Density determinations on core samples of volcanic rocks from wells Z-11, Z-2, and ZCQ-2 varied from 2.07 to 2.43 g/cm^3 and averaged 2.25 g/cm^3. Lower densities generally correspond to shallower depths. Nettleton profiles (Telford et al., 1976) computed for Lines 2, 3, 7, and 8 also indicated that densities of 1.9 to 2.3 g/cm^3 were most appropriate for Bouguer and terrain corrections.

Terrain-corrected Bouguer gravity maps were prepared for densities of 2.00, 2.20, 2.30, and 2.67 g/cm^3 and correlated with topography. The 2.20 and 2.30 g/cm^3 Bouguer anomaly maps were judged to be most appropriate for interpretation and a linear regional gradient of -5 mGal/km (N45°E) was removed from these maps to form residual anomaly maps. The residual anomaly maps for densities of 2.20 and 2.30 g/cm^3 are very similar. The 2.30 g/cm^3 map is shown in Figure 4.

Topographic corrections are extreme in the Zunil gravity data. Numerous topographic corrections exceed 12 mGal, with a maximum correction of 13.6 mGal for a density of 2.30 g/cm^3. The difference in terrain corrections exceeds 3.0 mGal for adjacent stations at several locations. An error of 10 to 30 percent is common in estimating terrain corrections in cases of severe topography, suggesting a possible error of 1 to 4 mGal from inaccuracies in terrain corrections alone. The contoured Bouguer gravity maps suggest an error level generally less than this but it is apparent that the possible error range for topographic corrections alone exceeds the amplitude of anomalies of interest in the well field at Zunil.

The residual anomaly map shows a lower correlation between the low gravity values and high topography west and north of the well field compared to the Bouguer anomaly maps. Northeast- and northwest-trending maxima and minima that are not present in the Bouguer gravity maps, are well defined on the residual anomaly maps and are more suitable for interpretation.

A structural interpretation of the data was completed by delineating discontinuities in the residual anomaly map. Areas of steep gradients having continuity between survey lines, and the termination of anomaly patterns, are interpreted as indications of faults. The low relief in the gravity data compared to the estimated noise level due to terrain corrections and other survey errors introduces some uncertainty in the interpretation. A simple, semi-quantitative estimate of the maximum depth to the source of a gravity anomaly is given by the breadth of the steep linear-gradient portion of gravity anomaly. For the anomalies in Figure 4, most of the linear-gradient distances are quite short, generally less than 300 m, indicating that density differences occur at shallow depths.

A number of three-dimensional gravity models was computed to assist in an interpretation of the residual anomaly map. Models were computed which simulated up to 500 m offset due to faulting of the grandodiorite (density 2.67 g/cm^3) at depths of 500 m to 1400 m. These models demonstrate that the gravity expression of such faulting is too small in amplitude for reliable interpretation. However, density contrasts of -0.30 to +0.10 g/cm^3 with respect to a background density of 2.30 g/cm^3, at depths of 0 to 500 m, give rise to gradient patterns and anomaly amplitudes similar to those observed in Figure 4. A complex model consisting of 30 prism sources to represent known depth variations in the granodiorite and near surface density variations in the overlying volcanics duplicated the amplitudes (-3 to +1 mGal) and main contour patterns observed in Figure 4. The steep gradients of 100 to 200 m width can only be explained by shallow density variations.

Interpreted structures and areas of denser volcanic rocks are superposed on the residual gravity map in Figure 4. The agreement with mapped structures is good considering the noise level of the gravity data, the distance between survey lines, and the station spacing of 70 to 200 m. The northeast-trending zone of denser volcanic rock indicated by the gravity interpretation includes wells ZCQ-2,3,4,5 and 6 which all display intense hydrothermal alteration and silicification.

SUMMARY

The Zunil geothermal system is developed in a complex sequence of young volcanic tuffs, breccias, and flows that is underlain by highly fractured granodiorite. Geologic mapping suggests that the location of the field is related to the intersection of a regional northeast-trending fracture system with the ring structure of a large caldera. The caldera is now largely filled by younger volcanic rocks. Evidence for the existence of this caldera includes the occurrence of a large circular feature visible on satellite images, the presence of thick sequences of ash-flow tuffs with no known source area, and the occurrence of ash-flow tuffs near the base of the volcanic sequence in the production wells.

Fluid production within the well field is controlled by northwest and northeast-trending faults that are reflected in both the topography and the gravity data. A shallow upflow zone, defined by chemical and thermal data, is located at the intersection of these structures near the western margin of the well field. Temperatures as high as 288°C have been encountered in this portion of the field at depths of 1000 m.

Hydrothermal alteration within the production wells, which range from 872 to 1310 m in depth, generally increases downward. Two distinct types of alteration assemblages have been observed in the deeper parts of the wells. The upwelling fluids have produced veins containing varying proportions of quartz, calcite, epidote, and wairakite and have cemented hydrothermal breccias with quartz and calcite.

Steam and gas derived from the upwelling fluids has led to the development of secondary steam-heated waters. These CO_2-enriched fluids have produced veins containing albite or illite and in places, intense illitization. The widespread occurrence of younger illite veins in rocks containing quartz + epidote + calcite veins suggests that the secondary steam-heated fluids are well-developed at Zunil and that they are currently migrating downward into the deeper portions of the system. The thickness of the steam-heated reservoir increases from west to east. K-Ar dating of a sample of the illite has yielded an age of $248 \pm 9 \times 10^3$ years.

Variations in the degree and characteristics of the hydrothermal alteration have strongly influenced the electrical and gravity responses of the system. Vertical electrical soundings define a shallow resistive basement that correlates most closely with a change in clay content of the volcanic rocks from conductive smectites to more resistive illites and chlorites. Conductivity-thickness products calculated from the data increase from the west to the east and south across the well field. These variations are consistent with a zone of upwelling in the western part of the well field. Gravity data define several highs within the field. These highs may reflect an increase in the shallow densities of the volcanic rocks due to hydrothermal alteration.

ACKNOWLEDGMENTS

This project could not have been completed without the support of our colleagues at the Instituto Nacional de Electricificacíon, Morrison-Knudsen Engineers and Cordon y Merida Ing. In particular we would like to thank Ing. Luis Merida and Dr. L. L. Mink. Discussions with Drs. William Rose, Grant Heikan, Wendell Duffield and Samuel Bonis on the caldera hypotheses were particularly helpful, but Foley accepts full responsibility for any errors that might arise in the caldera as depicted and discussed herein.

Funding for this project was provided by Morrison-Knudsen Engineers who, in partnership with Cordon y Merida Ings. is under contract to the Instituto Nacional de Electricificacíon of Guatemala. Additional funding for the preparation of this manuscript was provided by the Department of Energy under contract number DE-AC07-85ID12489, such support does not constitute an endorsement by the U.S. Department of Energy of the views expressed in this publication.

REFERENCES

Adams, M. C., Mink, L. L., Moore, J. N., White, L. D., and Caicedo A. A., 1990, Geochemistry and hydrology of the Zunil geothermal system, Guatemala.

Christiansen, R. L., and Hildreth, W., 1989, Voluminous rhyolitic lavas of broad extent on the Yellowstone Plateau (abstract): New Mexico Bureau of Mines and Mineral Resources, Bulletin 131, p. 52.

ELC-Electroconsult, 1980, Proyecto Zunil, Evaluacion del potencial del campo; Petrografia ignea y mineralogia de alteracion: report submitted to INDE, ZUN-D-5110, 11 p.

Goff, F., Gardner, J. N., Baldridge, W. S., Hulen, J. B., Nielson, D. L., Vaniman, D., Heikan, G., Dungan, M. A., and Broxton, D., 1989, Volcanic and hydrothermal evolution of Valles caldera and Jemez volcanic field, in, Chapin, C. E., and Zidek, J., Field excursions to volcanic terrains in the western United States, Volume 1: Southern Rocky Mountain region: New Mexico Bureau of Mines and Mineral Resources, Memoir 46, p. 381-434.

Inman, J. R., 1975, Resistivity inversion with ridge regression: Geophysics, v. 40, p. 798-817.

Johns, G. W., 1975, Geology of the Cerro Quemado volcanic dome complex, Guatemala: unpublished M. Sc. thesis, Michigan Technological University, Houghton, Michigan, USA, 124 p.

Menzies, A. J., Granados, E. E., Sanyal, S. K., Mink, L. L., Merida-I, L. Caicedo-A., A., 1990, An integrated test program for the definition of a high-temperature geothermal reservoir: a case study from the Zunil geothermal field, Guatemala: Geothermal Resources Council Transactions, in press.

Mink, L., Merida, L. and Caicedo, A., 1988, Zunil, Guatemala geothermal project (overview) and update): Geothermal Resources Council Transactions, v. 12, p. 185-192.

Moore, J. N., Lemieux, M. M., and Adams, M. C., 1990, The ocurrance of CO_2 enriched fluids in active geothermal systems: Data from fluid inclusions, 15th Annual Stanford Reservoir Conference, in press.

Newhall, C. G., 1987, Geology of the Lake Atitlan region, western Guatemala: Journal of Volcanology and Geothermal Research, v. 33, p. 23-55.

Rose, W. I., 1987, Santa Maria, Guatemala: bimodal soda-rich calc-alkalic stratovolcano: Journal of Volcanology and Geothermal Research, v. 33, p. 109-129.

Smith, R. B., and Braile, L. W., 1984, Crustal structure and evolution of an explosive silicic volcanic system at Yellowstone National Park, *in* Explosive Volcanism: Inception, Evolution, and Hazards: National Academy of Sciences, Geophysics Study Committee, National Academy Press, Washington, D.C., p. 96-109.

Stoiber, R. E., and Carr, M. J., 1973, Quaternary volcanic and tectonic segmentation of Central America: Bulletin Volcanologic, v. 37, p. 304-325.

Telford, W. M., Geldart, L. P., Sheriff, R. E., and Keys, D. A., 1976, Applied Geophysics, Cambridge Univ. Press., 860 p.

Tobias G. E., 1978, Zunil project: prefactibility study. Geologic inform: exploratory boreholes of small diameter.

Tobias, E., and Quiesa, S., 1981, Mapa Geologica: INDE, Campo Geotermico de Zunil, Mayo, map.

Williams, H., 1960, Volcanic history of the Guatemalan highlands: University of California Publications in Geological Sciences, n. 38, p. 1-87.